JACS
JOURNAL OF THE AMERICAN CHEMICAL SOCIETY
Article
pubs.acs.org/JACS

Unveiling Secrets of Overcoming the "Heteroatom Problem" in Palladium-Catalyzed Aerobic C−H Functionalization of Heterocycles: A DFT Mechanistic Study

Yanfeng Dang,[†,‡] Xi Deng,[†] Jiandong Guo,[†] Chunyu Song,[†] Wenping Hu,[‡,§] and Zhi-Xiang Wang*[,†,§]

[†]School of Chemistry and Chemical Engineering, University of the Chinese Academy of Sciences, Beijing 100049, China
[‡]Department of Chemistry, School of Science, Tianjin University, Tianjin 300072, China
[§]Collaborative Innovation Center of Chemical Science and Engineering, Tianjin 300072, China

Supporting Information

ABSTRACT: Directed C−H functionalization of heterocycles through an exocyclic directing group (DG) is challenging due to the interference of the endocyclic heteroatom(s). Recently, the "heteroatom problem" was circumvented with the development of the protection-free Pd-catalyzed aerobic C−H functionalization of heterocycles guided by an exocyclic CONHOMe DG. We herein provide DFT mechanistic insights to facilitate the expansion of the strategy. The transformation proceeds as follows. First, the $Pd_2(dba)_3$ precursor interacts with *t*-BuNC (L, one of the substrates) and O_2 to form the $L_2Pd(II)$-η^2-O_2 peroxopalladium(II) species that can selectively oxidize *N*-methoxy amide (e.g., PyCONHOMe) substrate, giving an active $L_2Pd(II)X_2$ (X = PyCONOMe) species and releasing H_2O_2. After *t*-BuNC ligand migratory insertion followed by a 1,3-acyl migration and association with another *t*-BuNC, $L_2Pd(II)X_2$ converts to a more stable C-amidinyl $L_2Pd(II)XX'$ (X′ = PyCON(*t*-Bu)C═NOMe) species. Finally, $L_2Pd(II)XX'$ undergoes C−H activation and C−C reductive elimination, affording the product. The C−H activation is the rate-determining step. The success of the strategy has three origins: (i) the *N*-methoxy amide DG can be easily oxidized *in situ* to generate the active $L_2Pd(II)X_2$ species via the oxidase pathway, thus preventing the destructive oxygenase pathway leading to stable *t*-BuNCO or the O-bridged dimeric Pd(II) species. The methoxy group in this amide DG greatly facilitates the oxidase pathway, and the tautomerization of *N*-methoxy amide to its imidic acid tautomer makes the oxidation of the substrate even easier. (ii) The X group in $L_2Pd(II)X_2$ can serve as an internal base to promote the C−H activation via CMD (concerted metalation-deprotonation) mechanism. (iii) The strong coordination ability of *t*-BuNC substrate/ligand suppresses the conventional cyclopalladation pathway enabled by the coordination of an endocyclic heteroatom to the Pd-center.

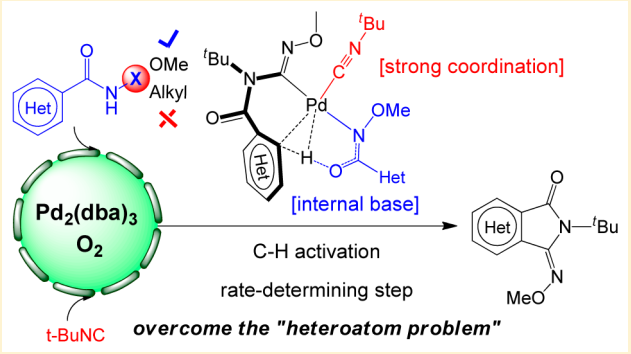

1. INTRODUCTION

The development of novel reactions to form C−C and C−heteroatom bonds for constructing complex molecular structures is a perpetual subject in organic synthesis.[1] A strategy currently pursued actively with great successes is directed C−H bond functionalization catalyzed by transition-metal (TM) complexes.[2−4] A key for the success of the strategy is that the substrate possesses an endogenous or exogenous heteroatom-containing directing group (DG) capable of docking an active TM species to selectively activate a specific C−H bond.[2] The strategy has promoted the developments of myriad C−H bond functionalization reactions, some of which have already been applied in drug or drug lead discoveries and natural product synthesis.[2] Unsatisfactorily, the methodology could be problematic in performing exocyclic DG-guided C−H bond functionalization of heterocycles, because an endocyclic heteroatom (e.g., N, O, S, and P) may disrupt the ligation of the exocyclic DG to the TM catalyst for targeted C−H bond functionalization, but diverse derivations of heterocycles are of great value in synthesizing pharmaceuticals, agrochemicals, and new materials.[5,6] To circumvent the "heteroatom problem", for example, in the Pd-catalyzed pyridine functionalization, Lewis acid or *N*-oxide formation was used to mortify the conventional cyclopalladation pathway guided by the endocyclic heteroatom of heterocycles; thus they were enabled to perform the desired allylic C−H functionalization.[7] Most recently, Dai, Yu, and their co-workers developed another remarkable strategy to overcome the problem, showcasing the exocyclic CONHOMe[8]-directed C−H functionalizations of various heterocycles (see Scheme 1 for examples).[9] The reactions used Pd(0) complex (e.g., $Pd_2(dba)_3$) as a catalyst precursor and air (O_2) as the sole oxidant, with no additives and no care for the endocyclic heteroatom(s), furnishing products with high yields (up to

Received: November 19, 2015
Published: February 4, 2016

DOI: 10.1021/jacs.5b12112
J. Am. Chem. Soc. 2016, 138, 2712−2723

Scheme 1. Palladium-Catalyzed Aerobic C−H Functionalization of Heterocycles and Arenes

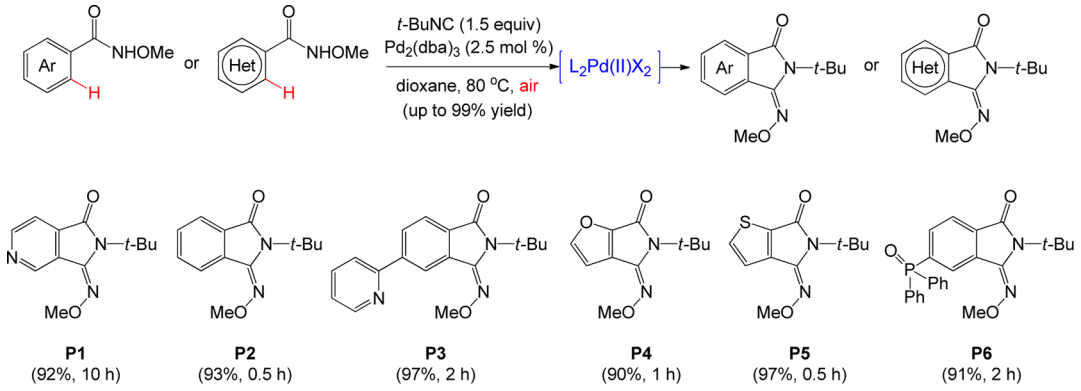

99%), and water as only byproduct. These transformations exemplify an ideal scenario in terms of "green" and atom-economic synthesis.[10,11] Undoubtedly, the strategy could be further exploited in other C−H bond functionalization transformations, as prospected by the experimentalists.[9] To expand the strategy, it is valuable to deeply understand the catalytic mechanism and the causes for overcoming the "heteroatom problem". Herein, we present a DFT mechanistic study to gain insight into the strategy according to structures and energetics which are often difficult to access experimentally, in the hope of taking the full advantage of the strategy.

In terms of mechanistic understanding, the study attempts to gain insight into the following issues: (i) As a "green" and atom-economic approach, aerobic condition has been utilized in TM-catalyzed reactions, and H_2O_2 is known to be the reduced product of O_2, but the detailed mechanism remains unclear. Using a representative transformation as an example, we unveil how O_2 prompts the oxidation of Pd(0) to Pd(II), thus *in situ* generating the active Pd(II)X_2 species. There are two mechanisms, including oxidase and oxygenase, for O_2 acting as an oxidant,[11] while the present transformation requires O_2 to selectively oxidize the *N*-methoxy amide substrate via oxidase pathway. It is of significance to understand why O_2 does not follow oxygenase mechanism to oxidize *t*-BuNC substrate (an analog of monoxide) giving Pd═O and *t*-BuNCO species. (ii) The *N*-methoxy amide substrates contain heterocyclic substituents such as pyridine and phenylpyridine, and the catalytic system also involves Pd(II) species (see Scheme 1). Intriguingly, the endocyclic heteroatom(s) does not disturb the effectiveness of the exocyclic CONHOMe DG at all, even in the case of **P3**, where the *para*-(2-pyridyl)benzamide reactant contains a phenylpyridine motif that is well-known to be a powerful DG to guide aryl C−H bond functionalization,[2] encouraging us to disclose the root-causes for overcoming the "heteroatom problem".

2. COMPUTATIONAL METHODS

Actual catalysts and substrates were employed in performing all standard DFT computations. Geometries were optimized and characterized by frequency analysis calculations to be minima or transition states (TSs) at B3LYP[12]/BSI level in the gas phase, where BSI denotes a basis set combining SDD[13] for palladium and 6-31G(d,p) for nonmetal atoms. The energies were then improved by M06-L[14]/BSII//B3LYP//BSI single-point energy calculations with solvent effects simulated by the SMD[15] solvent model, using the experimental solvent (dioxane). BSII denotes a mixed basis set of SDD for palladium and 6-311++G(d,p) for nonmetal atoms. The combined use of two DFT functionals has been successfully applied to investigate various TM-catalyzed reactions.[16,17] The refined energies were corrected to enthalpies and free energies at 298.15 K and 1 atm, using the gas phase B3LYP/BSI harmonic frequencies. Free energies (in kcal/mol) obtained from the M06-L/BSII//B3LYP/BSI calculations were discussed. The location of MECP (minimum energy crossing point) was performed by using the location program developed by the Harvey group.[18] All DFT calculations were carried out with Gaussian 09 program.[19] Additional computational results are given in Supporting Information.

3. RESULTS AND DISCUSSION

3.1. Catalytic Route Leading to the Product. Dai, Yu, and co-workers have demonstrated their strategy to be effective in functionalizing various heterocycles. We chose the reaction in eq 1 as a representative to probe the mechanism, because the

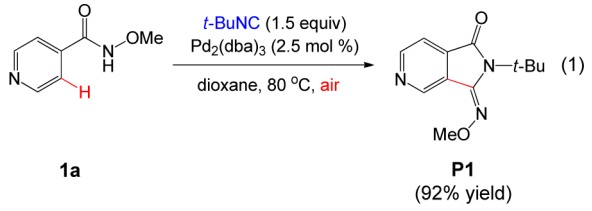

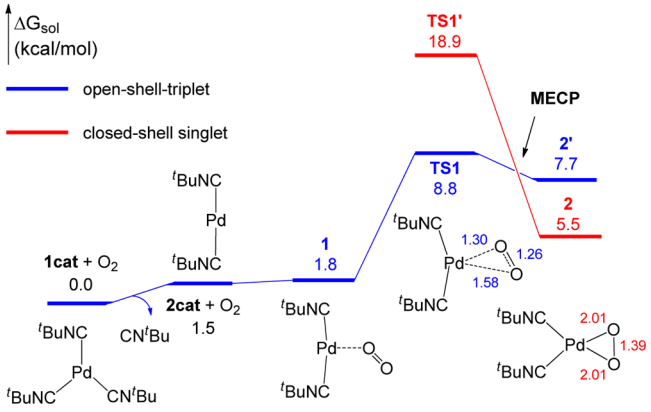

Figure 1. Free energy profiles for the oxygenation of **2cat** giving peroxopalladium(II) species **2**. Energies are relative to **1cat** + O_2 (triplet) and are mass balanced.

N-methoxy amide substrate **1** contains a typical heterocyclic pyridine substituent. The catalytic system used $Pd_2(dba)_3$ as Pd(0) source. Under the consideration of the components available in the catalytic system, we examined various routes possibly leading to a Pd(0) monomer (see Figure S1) and found that the generation of (*t*-BuNC)$_3$Pd(0) species (**1cat**)

DOI: 10.1021/jacs.5b12112
J. Am. Chem. Soc. 2016, 138, 2712−2723

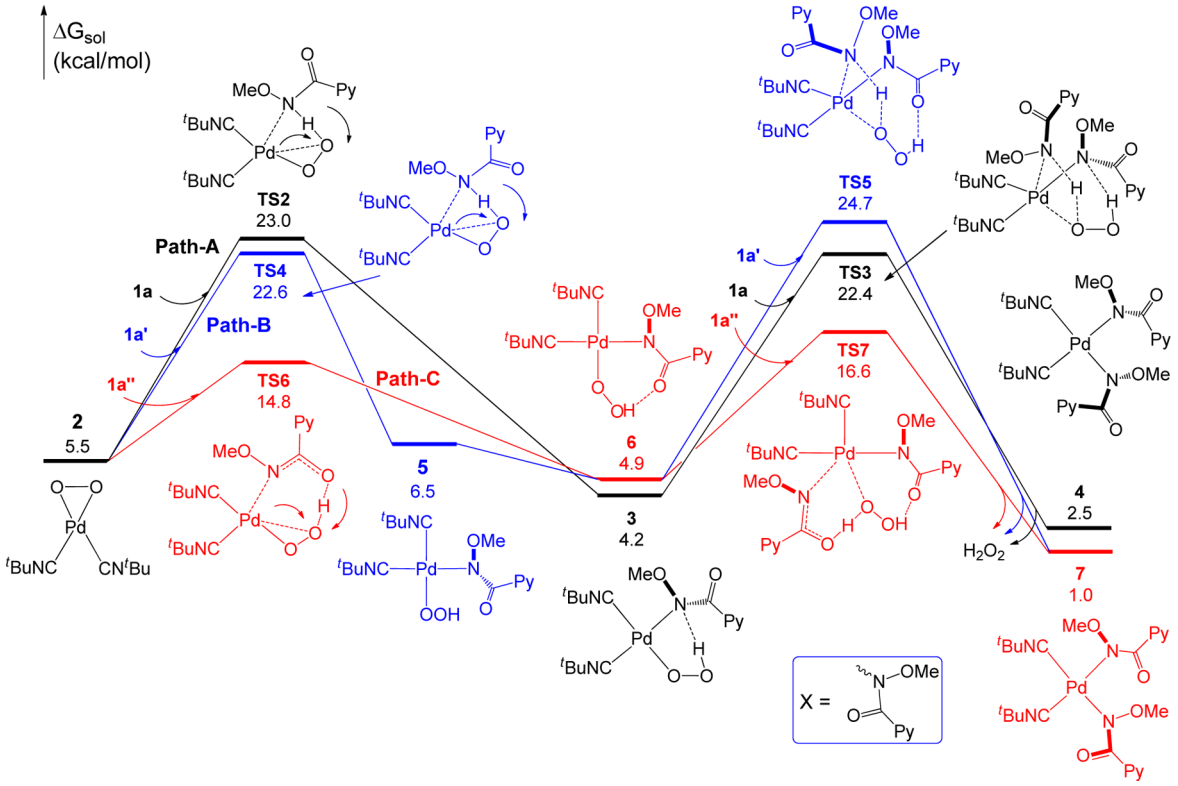

Figure 2. Free energy profiles for the oxidation of *N*-methoxy amide **1a** to give the active Pd(II)X_2 species **4** and **7**. Energies are relative to **1cat** + O_2 (triplet) and are mass balanced.

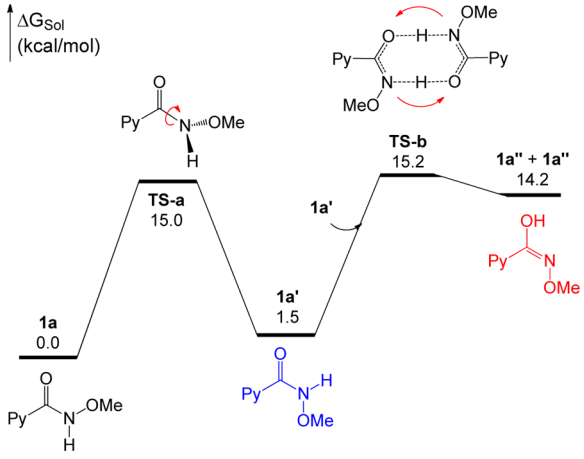

Figure 3. Free energy profile for the tautomerization of amide **1a** to imidic acid **1a**″. Energies are relative to substrate **1a** and are mass balanced.

was most thermodynamically favorable with an energy release of 5.1 kcal/mol (eq 2); thus **1cat** was used to initiate the catalysis and also as the energy reference together with the most stable reactants (*t*-BuNC, **1a**, and O_2).

$$\frac{1}{2}Pd_2(dba)_3 + 3(t\text{-BuNC}) \xrightarrow[\Delta G=-5.1\ \text{kcal/mol}]{} (t\text{-BuNC})_3Pd + \frac{3}{2}dba \quad (2)$$

The reaction of $L_nPd(0)$ (L = NHC or other ligands) with O_2 involved in the aerobic palladium catalysis has been documented experimentally[11,20,21] and computationally.[22,23] It is generally concluded that the reaction produces a singlet peroxopalladium(II) intermediate as a key species to carry out catalysis. Figure 1 illustrates a similar mechanism for the reaction of **2cat** and O_2, leading to the singlet Pd(II)-peroxo complex **2** (see Figures S2 and S3 for more details). Its triplet counterpart **2**′ stemming from the interaction of **2cat** with triplet O_2 ground state is 2.2 kcal/mol higher than **2**; thus **2** is generated via intersection between singlet and triplet energy surfaces, as identified by the located MECP (see Figure S4). Compared to the bond length (1.22 Å) of free O_2, the O_2 moiety in **2** is stretched to 1.39 Å, which can be attributed to the donation of Pd d_{xy} electrons to the O_2 π_{xy}* orbital. Because *t*-BuNC is a weaker electron donating ligand than NHC, unlike the exergonic reaction of $(NHC)_2Pd(0)$ with O_2,[22] **2** is 4.0 kcal/mol higher than **2cat** + O_2.

Figure 2 shows that once the Pd(II)-peroxo species **2** is attained, substrate **1a** attacks the Pd(II) center of **2** in a manner depicted by **TS2** (Path-A), transferring its H(−N) atom to the O−O moiety and concomitantly forming Pd−N covalent bond. The H(−N) deprotonation spans an energy barrier of 23.0 kcal/mol and gives Pd(II) hydroperoxide species **3**. Subsequently, another **1a** interacts with **3** through **TS3**, which transfers the H(−N) atom of **1a** to −OOH ligand of **3**, resulting in a *cis*-Pd(II)X_2 (X = PyCONOMe) species **4** and releasing H_2O_2. Hydrogen peroxide has been reported to be the byproduct of O_2 reduction in Pd-catalyzed aerobic catalytic reactions and can undergo disproportionation (i.e., $H_2O_2 \rightarrow H_2O + 1/2\ O_2$) resulting in water.[20e,21]

Essentially, **1a** is oxidized via transferring its H(−N) atom to O−O in **2** or OOH in **3** (Path-A). The overall barrier (**TS2**, $\Delta G^{\ddagger}$ = 23.0 kcal/mol) for the deprotonation process is not high, but the tautomerization between amide and imidic acid spurred us to ponder whether the H transfers can be accelerated by converting the amide **1a** to its imidic acid

DOI: 10.1021/jacs.5b12112
J. Am. Chem. Soc. 2016, 138, 2712−2723

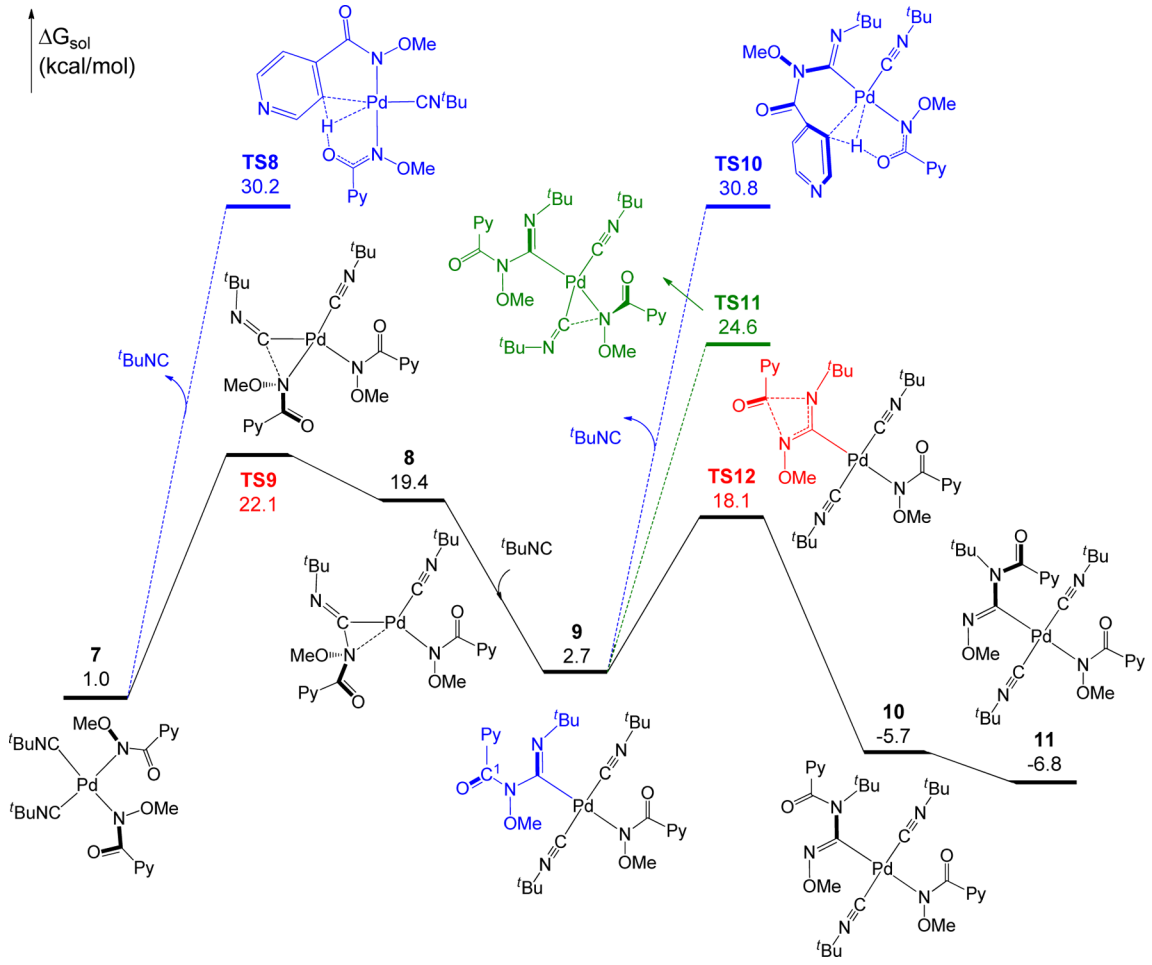

Figure 4. Free energy profile for the migratory insertion and acyl migration processes leading to the C-amidinyl Pd(II) complex **11**. Energies are relative to **1cat** + O_2 (triplet) and are mass balanced.

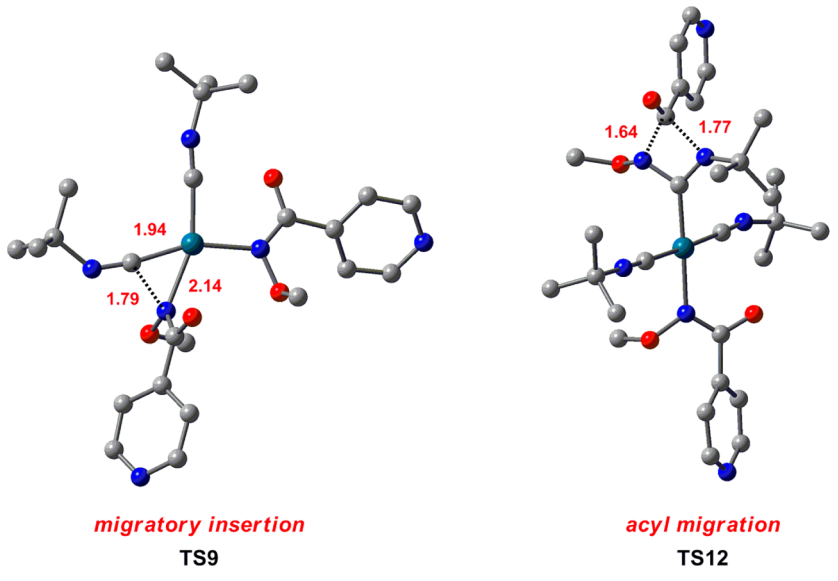

Figure 5. Optimized structures of **TS9** (1,1-migratory insertion) and **TS12** (1,3-acyl migration) with selected bond distances given in angstroms. H atoms are omitted for clarity.

tautomer **1a**″ (Figure 3), since the OH hydroxyl group in the imidic acid **1a**″ may lose H(−O) atom easier than H−N group in amide **1a**. Neither acid nor base was applied in the present transformation, we thus proposed that **1a** could be feasibly tautomerized to **1a**″ via a biomolecular mechanism described in Figure 3. First, **1a** rotates around the C−N bond with a barrier of 15.0 kcal/mol (**TS-a**), converting **1a** to the slightly less stable rotamer **1a**′. Then tautomerization proceeds via intermolecular

DOI: 10.1021/jacs.5b12112
J. Am. Chem. Soc. 2016, 138, 2712−2723

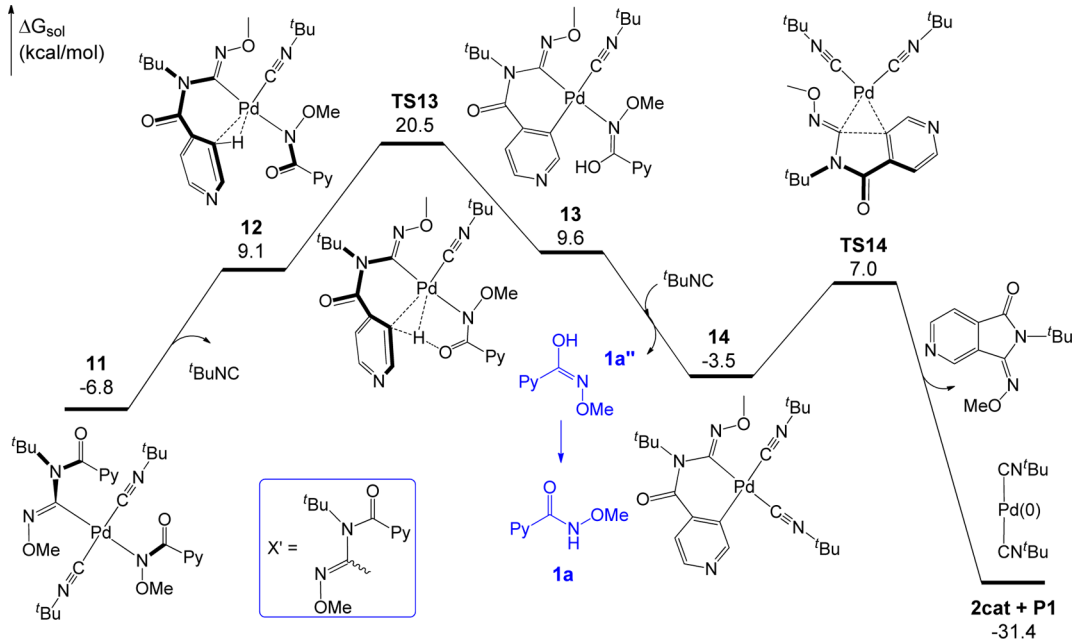

Figure 6. Free energy profile for the Pd(II)-mediated C−H activation and C−C reductive elimination, leading to the final product **P1** and regenerating the Pd(0) catalyst **2cat**. Energies are relative to **1cat** + O_2 (triplet) and are mass balanced.

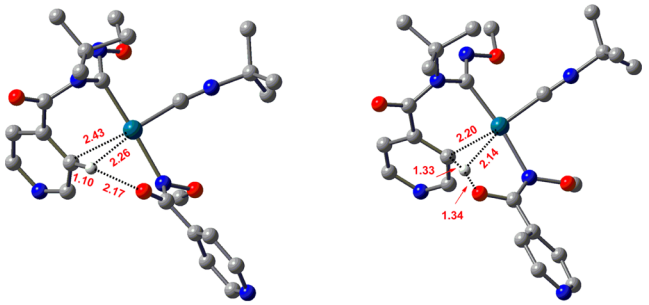

Figure 7. Optimized structures of **TS13** (C−H activation) and its precursor **12**, with selected bond distances given in angstroms. H atoms are omitted for clarity except those in question.

hydrogen exchanges of two **1a′** molecules via **TS-b** ($\Delta G^{\ddagger}$ = 15.2 kcal/mol), giving **1a″**. Note that the tautomerization mechanism cannot be applied to ketone-enol tautomerization, because, for example, the barrier for acetone tautomerization reaches as high as 61.6 kcal/mol. The significantly decreased barrier for **1a**−**1a″** tautomerization can be ascribed to the stronger protonic nature of H(−N) than H($-C_{sp3}$). The energetics indicates the kinetic feasibility of the tautomerization.

The reaction pathway of **2** with **1a″** is displayed in Figure 2 (the red pathway, Path-C). Fulfilling our expectation, **1a″** indeed reacts with **2** much easier; the highest barrier (**TS7**) along the red pathway is 6.4 kcal/mol lower than its counterpart (**TS2**) along the black pathway. In addition, the former is thermodynamically more favorable than the latter by 1.5 kcal/mol (ΔG(**7**) − ΔG(**4**)). It is worth pointing out that the energies of the stationary points along the red Path-C are also measured from the most stable **1a**; thus the thermodynamic disadvantage of **1a″** relative to **1a** is accounted. The explorations indicate that the tautomerization greatly facilitates the production of the active Pd(II)X_2 species and suggest that possible tautomerization should be considered in developing similar TM-catalyzed aerobic transformations.

We also considered the possibility of using rotamer **1a′** (Figure 3) to complete the hydrogen-transfer processes (Path-B). Compared to **1a** and **1a″** (Figure 2), **1a′** is inferior, though **1a′** has a pathway (see Figure S5) that is more favorable than the blue pathway (Path-B) in Figure 2. More possible oxidation pathways are excluded in Figure S6.

No matter which isomer (**1a**, **1a′**, or **1a″**) participates in the stage, the Pd(II)X_2 species is produced. The two X groups in **4** and **7** adopt a cis arrangement. Their trans isomers (*trans*-**4** and *trans*-**7**) are energetically comparable to these cis isomers, but the reaction pathways (see Figure S6 for details) to produce these *trans*-Pd(II)X_2 species are less favorable than those in Figure 2, due to lacking intramolecular hydrogen bonds. Furthermore, we examined whether **7** can be converted to a bidentate complex (i.e., LPd(II)X(κ^2-N(OMe)C═OPy)) after dissociating a *t*-BuNC ligand, but LPd(II)X(κ^2-N(OMe)C═OPy) + *t*-BuNC is 13.5 kcal/mol higher than **7**, excluding the possibility (see Figure S7 for more details).

We took the four Pd(II)X_2 species (**4**, **7**, *trans*-**4**, and *trans*-**7**) into consideration proceeding to the subsequent *t*-BuNC migratory insertion step and found that **7** is energetically most favorable. We below use **7** to illustrate the mechanism of the migratory insertion (Figure 4) and give the results of the other three scenarios in Figure S8.

Conventionally, Pd-directed C−H bond functionalizations use an external or internal base to perform C−H activation.[2m,s,v,24,25] Dai, Yu, and co-workers' strategy only used Pd(0) precursor, and no external base was added. Nevertheless, the X group in the *in situ* generated Pd(II)X_2 species **7** is akin to the carboxylate group;[2m] thus one of the two X groups, acting as an internal base, can extract the H(−C) atom of the other X group via the CMD (concerted metalation-deprotonation) mechanism. Indeed, we were able to locate **TS8** for the CMD process (Figure 4), but the C−H activation is not preferred. Due to the carbon-monoxide-like character of

DOI: 10.1021/jacs.5b12112
J. Am. Chem. Soc. 2016, 138, 2712−2723

Scheme 2. Catalytic Cycle for the Pd(0)/Pd(II)-Catalyzed Aerobic C−H Functionalization

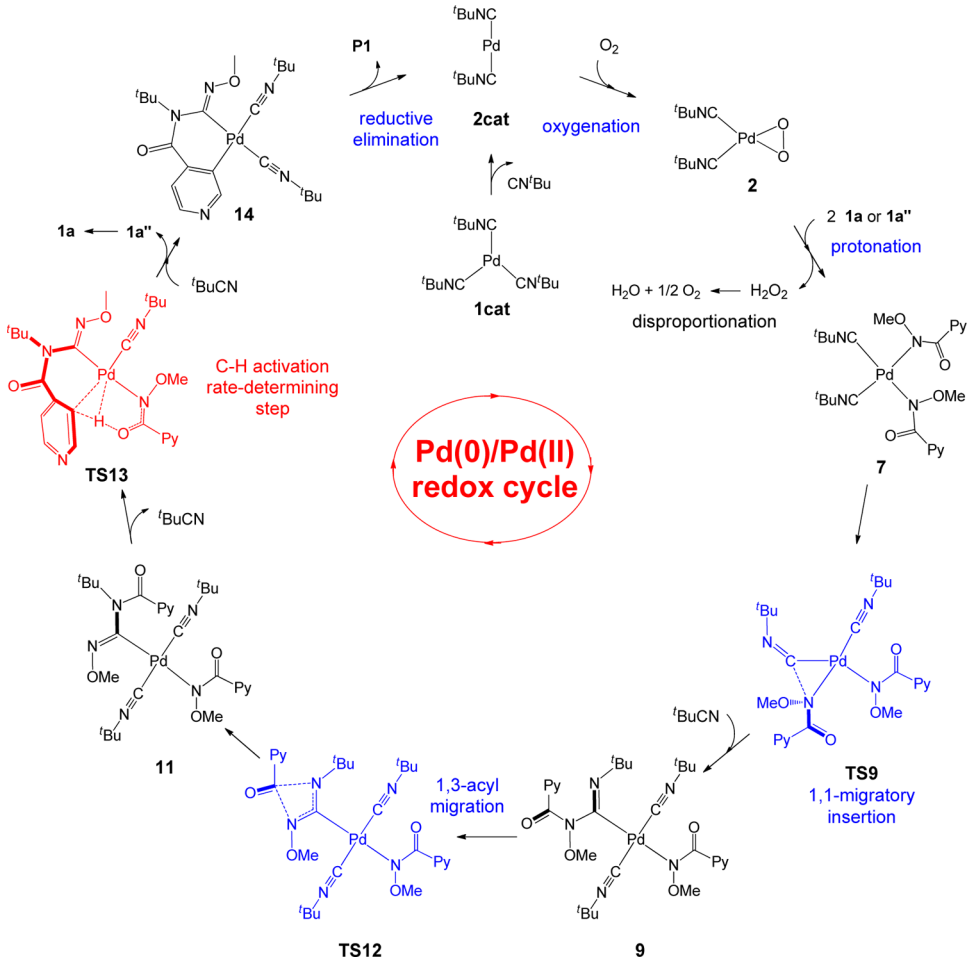

Table 1. Correlations Between Computed Rate-Determining C−H Bond Activation Barriers and Experimental Yields

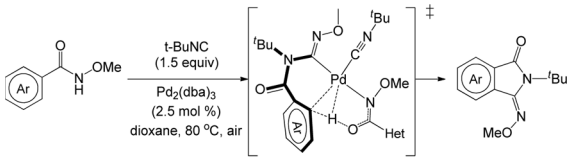

entry	Ar	$\Delta G^{\ddagger}_{RD}$[a]	yield (%)/time (h)
1	*p*-OMe-Ph−	23.4	97/0.5
2	*p*-Me-Ph−	24.9	96/0.5
3	Ph−	24.4	93/0.5
4	*p*-F-Ph−	25.0	98/6
5	*p*-Cl-Ph−	26.3	94/6
6	*p*-Br-Ph−	26.3	80%/6 h
7	*p*-MeO_2C-Ph−	26.5	87/3
8	*p*-CF_3−Ph−	27.3	78/6
9	*p*-CN-Ph−	28.8	79/6

[a]Energy barriers are given in kcal/mol.

isocyanide *t*-BuNC,[26] **7** favors undergoing intramolecular migratory insertion via **TS9** (see Figures 4 and 5), inserting a *t*-BuNC ligand into a Pd−N bond, resulting in **8**; the migratory insertion is 8.1 kcal/mol more favorable than the C−H bond activation (**TS8** vs **TS9**). The high C−H bond activation barrier (**TS8**) can mainly be attributed to the cost for dissociating a *t*-BuNC ligand (see section 3.2.2 for further discussion). Relative to **7**, the migration is kinetically favorable with a barrier of 21.1 kcal/mol (**TS9**) but thermodynamically unfavorable by 18.4 kcal/mol. Ultimately, the migration evacuates a vacant coordination site, allowing another *t*-BuNC substrate/ligand to ligate to the Pd(II) center to drive **8** down to much more stable **9**.

At a glimpse of the structure of **9**, one may think, similar to **7**, it could undergo migratory insertion to form C−N bond or C−H bond activation, as illustrated by **TS10** ($\Delta G^{\ddagger}$ = 30.8 kcal/mol) and **TS11** ($\Delta G^{\ddagger}$ = 24.6 kcal/mol), respectively. In spite of the accessible barriers, the two processes are not preferential. Because of the high electron deficiency of the carbonyl carbon (i.e., C^1) atom in complex **9**, the acyl group (PyC═O) favors undergoing a nucleophilic attack (or 1,3-acyl migration) through **TS12** (see Figures 4 and 5), transferring the electron-deficient acyl group from N(−OMe) to more nucleophilic N(−^{t}Bu) group to lead to the C-amidinyl Pd(II) species **10**. Subsequently, **10** rotates around the C−N single bond to turn the bulky *t*-Bu group away from the Pd center, resulting in a more stable C-amidinyl Pd(II) complex **11**. Kinetically, the 1,3-acyl migration is 6.5 and 12.7 kcal/mol more favorable than the *t*-BuNC migratory insertion and C−H activation, respectively. Relative to **9**, the 1,3-acyl migration is exergonic by 9.5 kcal/mol once **11** is reached.

Like **7** and **9**, **11** features a Pd−N covalent bond, *t*-BuNC ligands, and internal base (i.e., X^-); thus **11** may undergo either

DOI: 10.1021/jacs.5b12112
J. Am. Chem. Soc. 2016, 138, 2712−2723

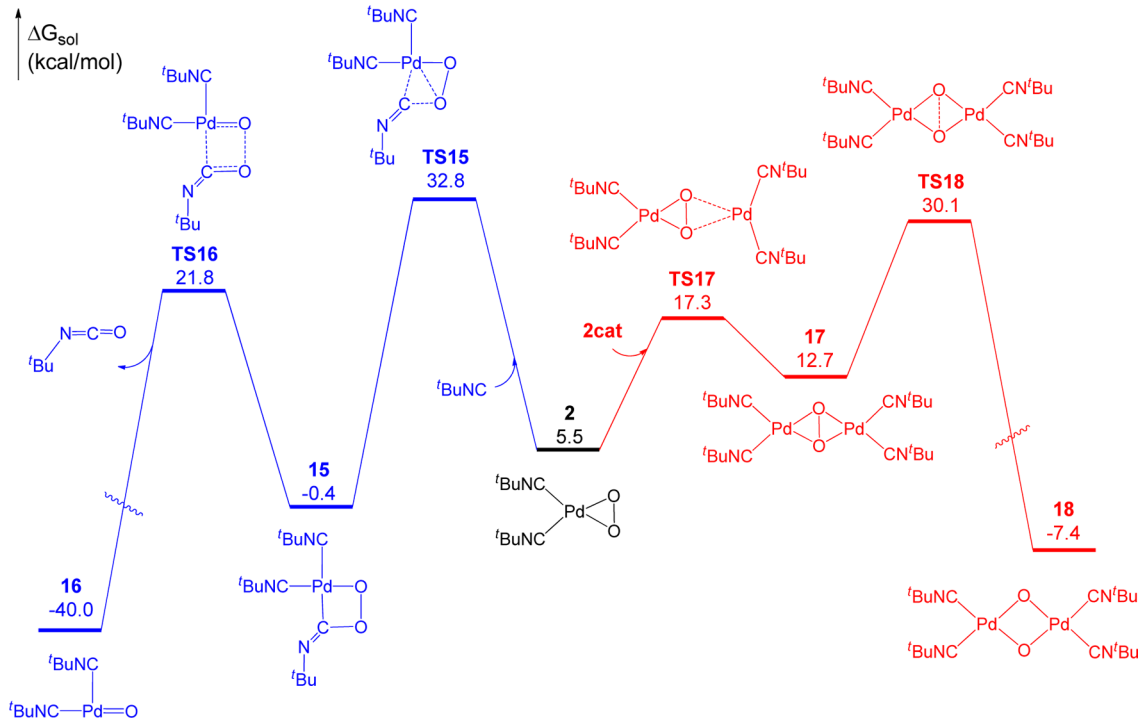

Figure 8. Free energy profiles for the possible side-pathways initiated from Pd(II)-peroxo species **2**. Energies are relative to **1cat** + O_2 (triplet) and are mass balanced.

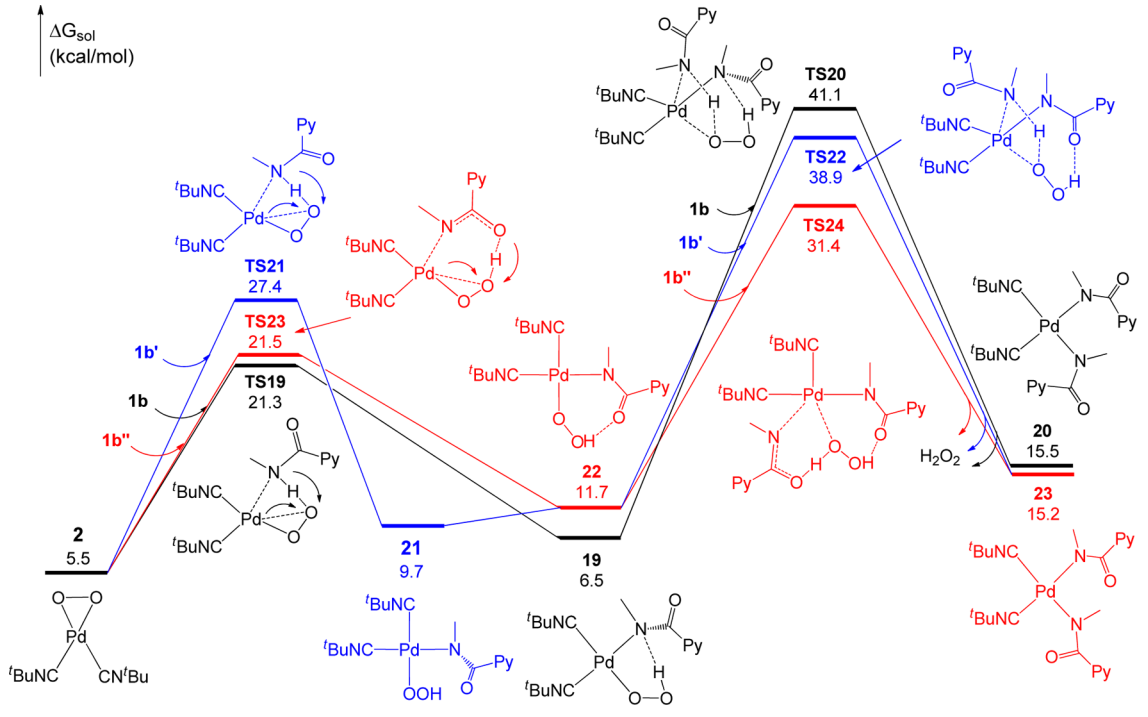

Figure 9. Free energy profiles for the oxidation of *N*-alkyl amide **1b** to give the Pd(II)X_2 (X = PyCONMe) species **20** and **23**. Energies are relative to **1cat** + O_2 (triplet) and are mass balanced.

t-BuNC migratory insertion or C−H bond activation. Unlike **7**, **11** prefers the latter (see Figure S9 for more details). The two anionic ligands (X^- and X'^- = -PyCON(*t*-Bu)C═NOMe) in **11** are separated by the *t*-BuNC ligands. To initiate the CMD C−H activation, one *t*-BuNC ligand is released with an energy increase by 15.9 kcal/mol, giving **12** that features a C−H agostic interaction. Subsequently, the amide C═O group of X^- ligand serves as an internal base to extract the H(−C) atom of X'^- by crossing **TS13**, giving **13**(Figure 6). The optimized structures of **TS13** and its precursor **12**, shown in Figure 7, confirm the CMD mechanism. The C−H bond activation converts the anionic X^- ligand to an L-type ligand (i.e., imidic acid **1a**″). Recall that **1a**″ is much easier to be oxidized than **1a** (see Figure 2). Because *t*-BuNC is stronger than **1a**″ in

DOI: 10.1021/jacs.5b12112
J. Am. Chem. Soc. 2016, 138, 2712−2723

Scheme 3. Pathways for Pd(II)-Catalyzed C−H Activation of *para*-(2-Pyridyl)benzamide (3a)[a]

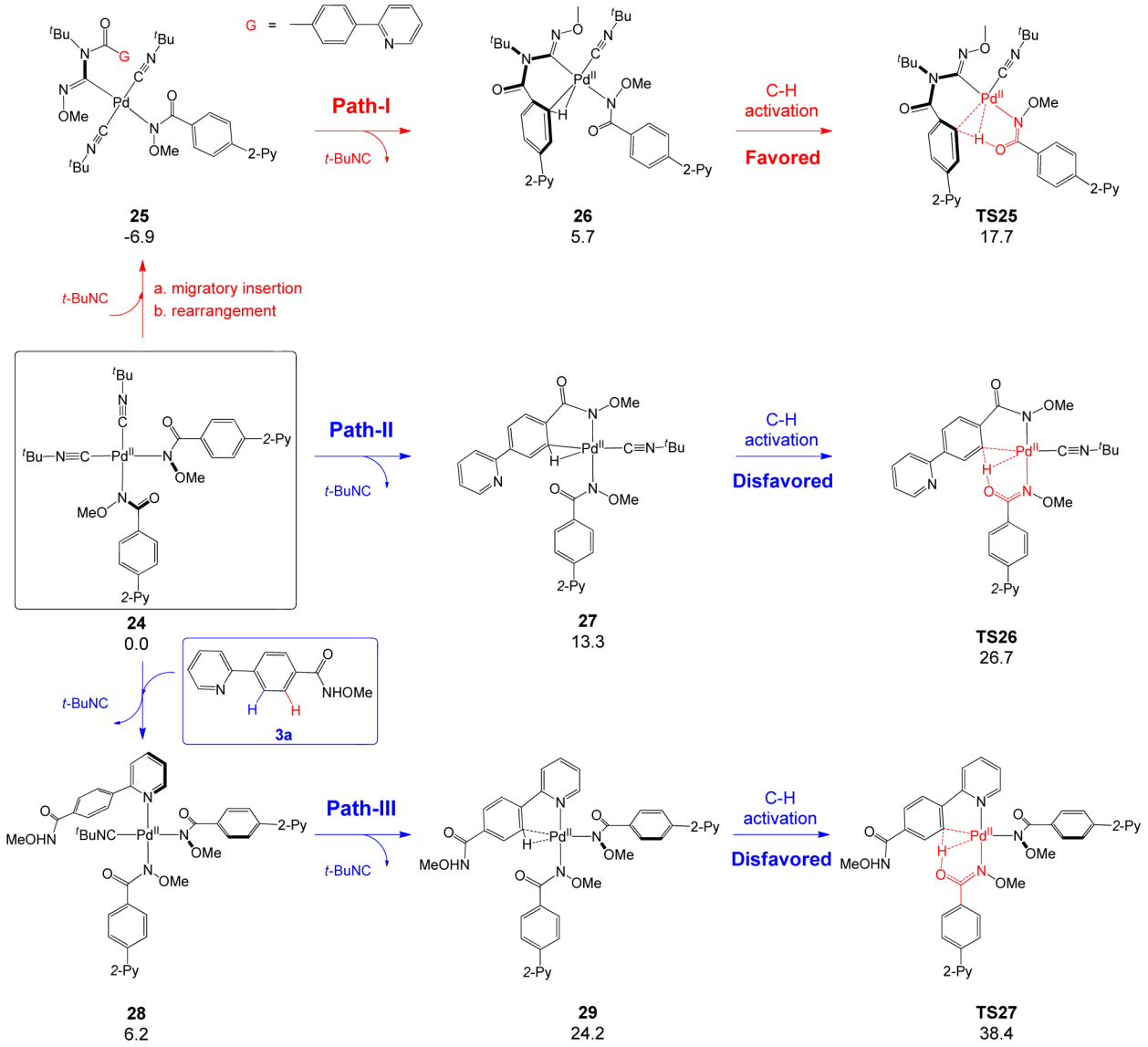

[a]Energies are relative to the active $L_2Pd(II)$ X_2 complex **24** and are mass balanced.

Scheme 4. Strong Coordination Ability of the *t*-BuNC Substrate/Ligand

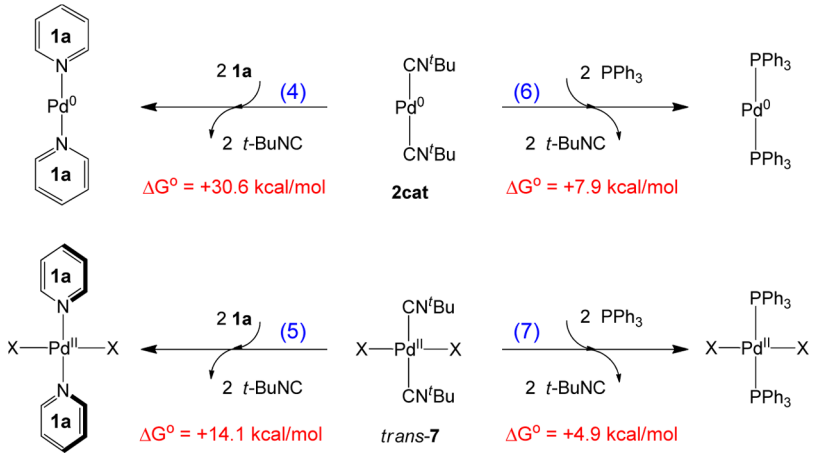

coordination to the Pd(II) center, *t*-BuNC exchanges with **1a**″ to drive **13** to more stable **14**. Eventually, **14** undergoes reductive elimination via **TS14** to form the C−C bond, affording the product (**P1**) and regenerating the Pd(0) species

DOI: 10.1021/jacs.5b12112
J. Am. Chem. Soc. 2016, 138, 2712−2723

(**2cat**). Note that **TS8**, **TS10**, and **TS13** all comply with the CMD mechanism to cleave the C−H bond. In Figure S10 we excluded the possible C−H oxidative addition mechanism via Pd(II)/Pd(IV) redox manifold with energy barriers higher than 39.7 kcal/mol.

To summarize, Scheme 2 sketches the complete catalytic cycle of the transformation. In the whole cycle, the Pd(II)-catalyzed amide-carbonyl-assisted C−H activation is the rate-determining step with a kinetic barrier of 27.3 kcal/mol (**TS13** relative to **11**) and the transformation is exergonic by 31.4 kcal/mol.[27] All possible side reactions are significantly less favorable. The energetic results well account for the experimental fact that the transformation gave product with high yield (92%) at elevated temperature (80.0 °C). The energetic results predict that **11** is the most stable Pd(II) species involved in the whole catalytic cycle (see Figures 1, 2, 4, and 6). Consistently, the species is structurally similar to the Pd(II) complex (i.e., species ***E*** in ref 9) characterized by X-ray crystallography which can be viewed as the product of Cl^- exchange with the anionic *N*-methoxy amide ligand in **11**. The agreement corroborates the hypothesis of experimentalists that the isolated intermediate as an active species could be involved in the catalytic cycle.

Experimentally, various derivatives of **1a** have been used to perform similar transformations. According to our computed mechanism, we focused on the rate-determining barriers (C−H activation) of these transformations and compared the barriers in Table 1. Generally, the electron-donating substitutents (e.g., entries 1−3) lead to relatively low barriers; thus these conversions took shorter time but with high yields. The reactions with electron-withdrawing substituents (e.g., entries 4−6) have relatively higher barriers, thus spending relatively more time to give comparable yields. The strong electron-withdrawing substituents (e.g., entries 7−9) have even higher barriers; thus these transformations took longer time but afforded less products. These computational results further corroborate that the Pd(II)-catalyzed C−H activation occurs via the amide-carbonyl-assisted CMD mechanism. Because the electron-donating substituents in arenes enhance the basicity of amide carbonyl group, the H-abstraction for C−H activation step by the amide carbonyl group became easier, and vice versa.

3.2. Origins for Overcoming the "Heteroatom Problem". Broadly saying, as proposed by the experimentalists and demonstrated by our computed catalytic cycle (Scheme 2), the transformation operates via *in situ* converting the Pd(0) precatalyst to an active $Pd(II)X_2$ species via aerobic reaction with amide substrates. The facile formation of covalent Pd−N bonds between amide substrates with palladium centers effectively inhibits the coordination of the Pd(0) species to the heteroatoms of heterocycles that could initiate endocyclic DG-guided C−H functionalization. After establishing the catalytic route, we now analyze the root-causes for overcoming the "heteroatom problem", including why the $Pd(II)X_2$ species could be generated and why the $Pd(II)X_2$ species could not promote the endocyclic DG-guided C−H functionalizations.

3.2.1. Preference for Oxidase over Oxygenase. In agreement with the original idea of Dai, Yu, and co-workers, our study demonstrates that a $Pd(II)X_2$ species (i.e., **7**) indeed participates in the catalysis (Scheme 2). In order to generate **7**, O_2 must selectively oxidize the *N*-methoxy amide substrate (e.g., **1a** in eq 1) through the oxidase pathway shown in Figure 2. However, the carbon-monoxide-like *t*-BuNC and Pd(0) species may also be oxidized, resulting in *t*-BuNCO and other Pd(II) species by following the oxygenase mechanism that is often adopted in the biological systems. Thus, a primary cause for overcoming the "heteroatom problem" should be the preference for oxidase over oxygenase.

To understand the preference, Figure 8 characterizes two possible oxygenase pathways. The left part of Figure 8 describes the oxidation of *t*-BuNC to *t*-BuNCO by **2** (an oxidizing species). First, *t*-BuNC attacks **2** via **TS15**, forming a four-membered intermediate **15**. Subsequently, O−O bond in **15** breaks via **TS16**, resulting in a Pd═O species **16** and releasing isocyanate *t*-BuNCO. Alternatively (the right part of Figure 8), another **2cat** interacts with **2** via **TS17**, forming **17**. Further electron donation from **2cat** to O−O π^* orbital breaks O−O bond, giving the oxygen-bridged **18**. Compared to the oxidase pathway in Figure 2, the oxygenase pathways are thermodynamically more favorable by 41.0 and 8.4 kcal/mol, but they are not kinetically competitive with the oxdiase pathway; the highest TSs of the two pathways, **TS15** ($\Delta G^{\ddagger}$ = 32.8 kcal/mol) and **TS18** ($\Delta G^{\ddagger}$ = 30.1 kcal/mol), are significantly higher than the highest TS (**TS7**, $\Delta G^{\ddagger}$ = 16.6 kcal/mol) of oxidase pathway. Furthermore, **TS15** and **TS18** are much higher than **TS9**, **TS12** (Figure 4), **TS13**, and **TS14** (Figure 6), thus ensuring the destructive oxygenase oxidations would not occur in the catalytic system.

3.2.2. The Role of the Methoxy Substituent in N-Methoxy Amide Directing Group. The energetics discussed above show the preference for oxidase over oxygenase. The question now becomes why this is the case. Examining the reactions reported in ref 9, we noted that all amide substrates contain *N*-methoxy amide groups as a directing groups;[28] however *N*-alkyl amide groups have also been used as a DG to perform directed C−H bond functionalization reactions.[29] On the basis of our computed mechanism and the identity of experimental substrates, we speculated that the methoxy group could play a role in enabling the oxidase pathway to produce the key active $Pd(II)X_2$ species **7**, because the methoxy group draws electrons from the bound nitrogen to enhance the protonic nature of H(−N) for its transfer. To affirm this, we replaced the methoxy group in **1a** with a methyl group (giving **1b**) to compute the oxidase pathway. Comparing Figure 9 with Figure 2, it is obvious that the oxidations of the *N*-methyl amide isomers (**1b**, **1b**′, and **1b**″) are much less favorable than that of any *N*-methoxy isomer (**1a**, **1a**′, or **1a**″) in terms of both kinetics and thermodynamics. Specifically, the rate-determining barrier along the most favorable pathway in the *N*-methyl amide case is 31.4 kcal/mol (**TS24**), much higher than the 16.6 kcal/mol (**TS7**) in the *N*-methoxy amide case. The oxidation of *N*-methoxy group is slightly exergonic by 0.6 kcal/mol (**6** relative to **2**) or 3.9 kcal/mol (**7** relative to **6**), while the oxidation of *N*-methyl amide is endergonic by 6.2 kcal/mol (**22** relative to **2**) or 3.5 kcal/mol (**23** relative to **22**). The energetic comparisons pronounce the pivotal role of the *N*-methoxy groups in promoting the production of the active $Pd(II)X_2$ species **7**. Besides, the tautomerization between **1b** and **1b**″ is highly unfavorable ($\Delta G^{\ddagger}$ = 29.5 kcal/mol and ΔG(**1b**″) − ΔG (**1b**) = 18.5 kcal/mol (see Figure S11 for more details)). Furthermore, the most favorable oxidase pathway of *N*-methyl amide group via **TS24** ($\Delta G^{\ddagger}$ = 31.4 kcal/mol) is even slightly less favorable than the oxygenase pathway via **TS18** ($\Delta G^{\ddagger}$ = 30.1 kcal/mol); thus, if *N*-methyl amides are used, the oxgenase pathway would override the formation of the active $Pd(II)X_2$ species.

The comparative study demonstrates that the *N*-methoxy amide DG plays a pivotal role in enabling the aerobic transformations via oxidase pathways. We propose that the

DOI: 10.1021/jacs.5b12112
J. Am. Chem. Soc. 2016, 138, 2712−2723

substituent of amide N should be electron-withdrawing to favor the oxidase pathway for facile generation of the active $Pd(II)X_2$ species.

3.2.3. The Role of the Strong Binding of Isocyanide t-BuNC. The active $Pd(II)X_2$ species **7** is similar to $Pd(II)(OAc)_2$. It has been reported that $Pd(OAc)_2$ could catalyze various aryl C−H functionalizations,[24,25] thus raising a question why the similar $Pd(II)X_2$ species does not promote aryl C−H bond functionalization through the guidance of endocyclic heteroatom(s). For this purpose, the reaction shown in eq 3

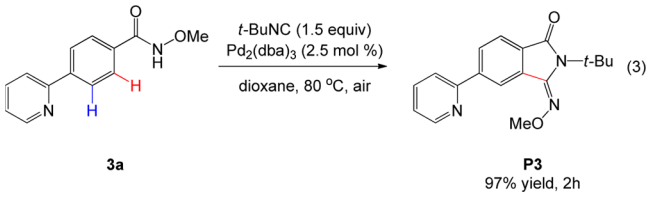

3a **P3** 97% yield, 2h

was considered to be an ideal case, because the 2-phenylpyridine motif in **3a** (*para*-(2-pyridyl)benzamide) strongly prefers pyridine nitrogen (N_{Py})-directed *ortho*-C−H bond (in blue) functionalizations via conventional cyclopalladation pathway.[2,30]

To understand why the N_{Py}-guided C−H functionalization (i.e., the heteoatom problem) did not occur under the present catalytic condition, we searched for the possible N_{Py}-directed cyclopalladation pathways to activate the C−H bond. Path-III in Scheme 3 represents the most likely pathway to perform the N_{Py}-directed C−H bond activation (see Figure S10 for other possibility). For comparisons, we also include Path-I which proceeds along the catalytic cycle shown in Scheme 2 (see Figure S12 for details) and Path-II which activates a C−H bond in X ligand directly. Comparing the three pathways, Path-I is most favorable with a rate-determining barrier (C−H activation) of 24.6 kcal/mol, in agreement with the experimental report that the CONHOMe-guided C−H bond functionalization gave **P3** in 97% yield.

Path-III uses **24** (the counterpart of **7**) as a Pd(II) species to activate an incoming **3a**. To begin with, **24** first dissociates a *t*-BuNC ligand to dock **3a** to the Pd(II) center of **24**, forming **28**. After further releasing the remaining *t*-BuNC ligand in **28** to allow interaction of the C−H bond (in red) with Pd(II) center, the resulting **29** proceeds to cleave the C−H bond via **TS27**. The energetic results given in Path-III indicate that the high **TS27** ($\Delta G^{\ddagger}$ = 38.4 kcal/mol) majorly originates from the costly replacement of two *t*-BuNC ligands with **3a** (from **24** to **29**), which raises the energy of the system by 24.2 kcal/mol. This also explains why **TS27** is higher than **TS26** in Path-II, because Path-II needs to dissociate one *t*-BuNC ligand. Therefore, we propose that the stronger coordination ability of *t*-BuNC than pyridine is also an important factor to avoid the N_{Py}-guided C−H bond functionalization in **24**, thus contributing to success of the strategy in overcoming the "heteroatom problem". The preference of Path-I over Path-II is mainly due to the fact that the isocyanide migratory insertion and acyl migration processes drive the system down to **25** by 6.9 kcal/mol. Supportively, the C−H activation barrier via **TS26** ($\Delta G^{\ddagger}$ = 26.7 kcal/mol) is only 2.1 kcal/mol higher than the 24.6 kcal/mol from **25** to **TS25**, but **TS26** is actually 9.0 kcal/mol higher than **TS25**.

The stronger coordination ability of *t*-BuNC than N_{Py} is also reflected by the endergonic eqs 4 and 5 in Scheme 4, which rationalize that eq 1 also cannot undergo N_{Py}-directed C−H bond functionalization. Experimentally, it has been reported that $Pd(PPh_3)_4$ is equally effective to perform the transformation.[9] Consistently, the replacements of *t*-BuNC ligands with PPh_3 ligands were predicted to be thermodynamically unfavorable (eqs 6 and 7), indicating that the even stronger coordination ligand PPh_3 is not able to interpret the catalytic route shown in Scheme 2.

4. CONCLUSION

Dai, Yu, and co-workers recently developed a novel strategy to address the challenging C−H bond functionalization of heterocycles through exocyclic directing groups and developed the Pd-catalyzed aerobic C−H bond functionalization of various heterocycles guided by exocyclic *N*-methoxy amide (CONHOMe) directing group. In the hope of facilitating the expansion of the strategy, we performed a DFT mechanistic study to unravel how O_2 oxidizes the *N*-methoxy amide substrate and how the strategy can overcome the "heteroatom problem". The study shows that the transformation proceeds via the following course. First, the Pd(0) precursor (i.e., $Pd_2(dba)_3$) interacts with *t*-BuNC (L = *t*-BuNC) and O_2 to form a peroxopalladium(II) species (i.e., $L_2Pd(II)$-η^2-O_2) that then oxidizes the *N*-methoxy amide (e.g., PyCONHMe), forming the active $L_2Pd(II)X_2$ (X = PyCONMe) species and releasing H_2O_2. Subsequent to the *t*-BuNC ligand/substrate migratory insertion followed by a 1,3-acyl migration via nucleophilic attack, $L_2Pd(II)X_2$ converts to the more stable C-amidinyl $L_2Pd(II)XX'$(X′ = PyCON(*t*-Bu)C═NOMe) species. Finally, $L_2Pd(II)XX'$ undergoes C−H activation and C−C reductive elimination, leading to the product. Among these steps, the C−H activation is the rate-determining step.

The root-causes for the success of the strategy include: (i) the *N*-methoxy amide directing group can be easily oxidized *in situ* to generate the active $L_2Pd(II)X_2$ species, thus preventing the destructive oxygenase pathways which lead to stable *t*-BuNCO and the O-bridged dimeric Pd(II) species. The methoxy group in the amide DG plays a pivotal role to allow the oxidase pathway to take place, and the tautomerization of *N*-methoxy amide to its imidic acid tautomer (i.e., **1a** → **1a**″) makes the oxidase pathway even easier. (ii) The X group in $L_2Pd(II)X_2$ can serve as an internal base to promote the C−H bond activation via CMD (concerted metalation-deprotonation) mechanism. (iii) The strong coordination ability of *t*-BuNC substrate/ligand suppresses the conventional cyclopalladation pathway directed by the coordination of an endocyclic heteroatom to the Pd-center. We expect that the mechanistic insights could facilitate the further development of the strategy in the developing TM-catalyzed C−H bond functionalization and aerobic reactions.

■ ASSOCIATED CONTENT

Supporting Information

The Supporting Information is available free of charge on the ACS Publications website at DOI: 10.1021/jacs.5b12112.

Additional computational results, energies, and Cartesian coordinates of the optimized structures (PDF)

■ AUTHOR INFORMATION

Corresponding Author

*zxwang@ucas.ac.cn

Notes

The authors declare no competing financial interest.

DOI: 10.1021/jacs.5b12112
J. Am. Chem. Soc. 2016, 138, 2712−2723

■ ACKNOWLEDGMENTS

We acknowledge the support for this work by the National Science Foundation of China (Grant Nos. 21373216 and 21573233) and the National Basic Research Program of China (973 Program, 2015CB856500). We greatly appreciate the insightful suggestions of the anonymous reviewers which helped us to improve the study.

■ REFERENCES

(1) Selected reviews: (a) Stille, J. K. *Angew. Chem., Int. Ed. Engl.* **1986**, *25*, 508. (b) Miyaura, N.; Suzuki, A. *Chem. Rev.* **1995**, *95*, 2457. (c) Demeijere, A.; Meyer, F. E. *Angew. Chem., Int. Ed. Engl.* **1995**, *33*, 2379. (d) Beletskaya, I. P.; Cheprakov, A. V. *Chem. Rev.* **2000**, *100*, 3009. (e) Luh, T.-Y.; Leung, M.-K.; Wong, K.-T. *Chem. Rev.* **2000**, *100*, 3187. (f) Trost, B. M.; Crawley, M. L. *Chem. Rev.* **2003**, *103*, 2921. (g) *Metal-Catalyzed Cross-Coupling Reactions*, 2nd ed.; de Meijere, A., Diedrich, F., Eds.; Wiley-VCH: Weinheim, Germany, 2004. (h) Beccalli, E. M.; Broggini, G.; Martinelli, M.; Sottocornola, S. *Chem. Rev.* **2007**, *107*, 5318. (i) Surry, D. S.; Buchwald, S. L. *Angew. Chem., Int. Ed.* **2008**, *47*, 6338. (j) Martin, R.; Buchwald, S. L. *Acc. Chem. Res.* **2008**, *41*, 1461. (k) Hartwig, J. F. *Nature* **2008**, *455*, 314. (l) Xue, L.; Lin, Z. *Chem. Soc. Rev.* **2010**, *39*, 1692. (m) Partyka, D. V. *Chem. Rev.* **2011**, *111*, 1529. (n) Liu, C.; Zhang, H.; Shi, W.; Lei, A. *Chem. Rev.* **2011**, *111*, 1780. (o) Johansson, C. C. C. S.; Kitching, M. O.; Colacot, T. J.; Snieckus, V. *Angew. Chem., Int. Ed.* **2012**, *51*, 5062. (p) García-Melchor, M.; Braga, A. A. C.; Lledós, A.; Ujaque, G.; Maseras, F. *Acc. Chem. Res.* **2013**, *46*, 2626. (q) Chen, F.; Wang, T.; Jiao, N. *Chem. Rev.* **2014**, *114*, 8613. (r) Volla, C. M. R.; Atodiresei, I.; Rueping, M. *Chem. Rev.* **2014**, *114*, 2390. (s) Souillart, L.; Cramer, N. *Chem. Rev.* **2015**, *115*, 9410. (t) Cherney, A. H.; Kadunce, N. T.; Reisman, S. E. *Chem. Rev.* **2015**, *115*, 9587. (u) Shin, K.; Kim, H.; Chang, S. *Acc. Chem. Res.* **2015**, *48*, 1040.

(2) Selected reviews on transition-metal-catalyzed C−H bond functionalizations: (a) Godula, K.; Sames, D. *Science* **2006**, *312*, 67. (b) Seregin, I. V.; Gevorgyan, V. *Chem. Soc. Rev.* **2007**, *36*, 1173. (c) Alberico, D.; Scott, M. E.; Lautens, M. *Chem. Rev.* **2007**, *107*, 174. (d) Lewis, J. C.; Bergman, R. G.; Ellman, J. A. *Acc. Chem. Res.* **2008**, *41*, 1013. (e) Davies, H. M. L.; Manning, J. R. *Nature* **2008**, *451*, 417. (f) Chen, X.; Engle, K. M.; Wang, D. H.; Yu, J. Q. *Angew. Chem., Int. Ed.* **2009**, *48*, 5094. (g) Daugulis, O.; Do, H.-Q.; Shabashov, D. *Acc. Chem. Res.* **2009**, *42*, 1074. (h) Ackermann, L.; Vicente, R.; Kapdi, A. R. *Angew. Chem., Int. Ed.* **2009**, *48*, 9792. (i) Colby, D. A.; Bergman, R. G.; Ellman, J. A. *Chem. Rev.* **2010**, *110*, 624. (j) Mkhalid, I. A. I.; Barnard, J. H.; Marder, T. B.; Murphy, J. M.; Hartwig, J. F. *Chem. Rev.* **2010**, *110*, 890. (k) Lyons, T. W.; Sanford, M. S. *Chem. Rev.* **2010**, *110*, 1147. (l) Yeung, C. S.; Dong, V. M. *Chem. Rev.* **2011**, *111*, 1215. (m) Ackermann, L. *Chem. Rev.* **2011**, *111*, 1315. (n) Cho, S. H.; Kim, J. Y.; Kwak, J.; Chang, S. *Chem. Soc. Rev.* **2011**, *40*, 5068. (o) Engle, K. M.; Mei, T.-S.; Wasa, M.; Yu, J.-Q. *Acc. Chem. Res.* **2012**, *45*, 788. (p) Colby, D. A.; Tsai, A. S.; Bergman, R. G.; Ellman, J. A. *Acc. Chem. Res.* **2012**, *45*, 814. (q) Yamaguchi, J.; Yamaguchi, A. D.; Itami, K. *Angew. Chem., Int. Ed.* **2012**, *51*, 8960. (r) Rouquet, G.; Chatani, N. *Angew. Chem., Int. Ed.* **2013**, *52*, 11726. (s) Ackermann, L. *Acc. Chem. Res.* **2014**, *47*, 281. (t) Gao, K.; Yoshikai, N. *Acc. Chem. Res.* **2014**, *47*, 1208. (u) Noisier, A. F. M.; Brimble, M. A. *Chem. Rev.* **2014**, *114*, 8775. (v) Musaev, D. G.; Figg, T. M.; Kaledin, A. L. *Chem. Soc. Rev.* **2014**, *43*, 5009. (w) Guo, X.-X.; Gu, D.-W.; Wu, Z.; Zhang, W. *Chem. Rev.* **2015**, *115*, 1622. (x) Cheng, G.-J.; Zhang, X.; Chung, L. W.; Xu, L.; Wu, Y.-D. *J. Am. Chem. Soc.* **2015**, *137*, 1706. (y) Yang, L.; Huang, H. *Chem. Rev.* **2015**, *115*, 3468. (z) Cheng, C.; Hartwig, J. F. *Chem. Rev.* **2015**, *115*, 8946.

(3) (a) C−H Activation. In *Topics in Current Chemistry*; Yu, J.-Q., Shi, Z.-J., Eds.; Springer: Berlin, 2010; Vol. *292*. (b) Wang, D.-H.; Engle, K. M.; Shi, B.-F.; Yu, J.-Q. *Science* **2010**, *327*, 315. (c) Leow, D.; Li, G.; Mei, T.-S.; Yu, J.-Q. *Nature* **2012**, *486*, 518. (d) Tang, R.; Li, G.; Yu, J.-Q. *Nature* **2014**, *507*, 215. (e) He, J.; Li, S.; Deng, Y.; Fu, H.; Laforteza, B. N.; Spangler, J. E.; Homs, A.; Yu, J.-Q. *Science* **2014**, *343*, 1216.

(4) McNally, A.; Haffemayer, B.; Collins, B. S. L.; Gaunt, M. J. *Nature* **2014**, *510*, 129.

(5) Davies, I. W.; Welch, C. J. *Science* **2009**, *325*, 701.

(6) (a) Meanwell, N. A. *Chem. Res. Toxicol.* **2011**, *24*, 1420. (b) Ritchie, T. J.; Macdonald, S. J. F.; Young, R. J.; Pickett, S. D. *Drug Discovery Today* **2011**, *16*, 164. (c) Bryan, M. C.; Dillon, B.; Hamann, L. G.; Hughes, G. J.; Kopach, M. E.; Peterson, E. A.; Pourashraf, M.; Raheem, I.; Richardson, P.; Richter, D.; Sneddon, H. F. *J. Med. Chem.* **2013**, *56*, 6007. (d) Schönherr, H.; Cernak, T. *Angew. Chem., Int. Ed.* **2013**, *52*, 12256.

(7) Malik, H. A.; Taylor, B. L. H.; Kerrigan, J. R.; Grob, J. E.; Houk, K. N.; Du Bois, J.; Hamann, L. G.; Patterson, A. W. *Chem. Sci.* **2014**, *5*, 2352.

(8) Wang, D.-H.; Wasa, M.; Giri, R.; Yu, J.-Q. *J. Am. Chem. Soc.* **2008**, *130*, 7190.

(9) Liu, Y.-J.; Xu, H.; Kong, W.-J.; Shang, M.; Dai, H.-X.; Yu, J.-Q. *Nature* **2014**, *515*, 389.

(10) Selected reviews about the reactions of transition-metal complexes with molecular oxygen: (a) Sheldon, R. A.; Arends, I. W. C. E.; ten Brink, G.-J.; Dijksman, A. *Acc. Chem. Res.* **2002**, *35*, 774. (b) Punniyamurthy, T.; Velusamy, S.; Iqbal, J. *Chem. Rev.* **2005**, *105*, 2329. (c) Schultz, M. J.; Sigman, M. S. *Tetrahedron* **2006**, *62*, 8227. (d) Que, L.; Tolman, W. B. *Nature* **2008**, *455*, 333. (e) Boisvert, L.; Goldberg, K. I. *Acc. Chem. Res.* **2012**, *45*, 899. (f) Shi, Z.; Zhang, C.; Tang, C.; Jiao, N. *Chem. Soc. Rev.* **2012**, *41*, 3381. (g) McCann, S. D.; Stahl, S. S. *Acc. Chem. Res.* **2015**, *48*, 1756.

(11) Selected reviews of palladium-catalyzed reactions using O_2 as the oxidant: (a) Stahl, S. S. *Angew. Chem., Int. Ed.* **2004**, *43*, 3400. (b) Stoltz, B. M. *Chem. Lett.* **2004**, *33*, 362. (c) Stahl, S. S. *Science* **2005**, *309*, 1824. (d) Sigman, M. S.; Jensen, D. R. *Acc. Chem. Res.* **2006**, *39*, 221. (e) Gligorich, K. M.; Sigman, M. S. *Angew. Chem., Int. Ed.* **2006**, *45*, 6612. (f) Cornell, C. N.; Sigman, M. S. *Inorg. Chem.* **2007**, *46*, 1903. (g) Wendlandt, A. E.; Suess, A. M.; Stahl, S. S. *Angew. Chem., Int. Ed.* **2011**, *50*, 11062. (h) Campbell, A. N.; Stahl, S. S. *Acc. Chem. Res.* **2012**, *45*, 851. (i) Gligorich, K. M.; Sigman, M. S. *Chem. Commun.* **2009**, 3854. (j) Wu, W.; Jiang, H. *Acc. Chem. Res.* **2012**, *45*, 1736.

(12) (a) Lee, C. T.; Yang, W. T.; Parr, R. G. *Phys. Rev. B: Condens. Matter Mater. Phys.* **1988**, *37*, 785. (b) Becke, A. D. *J. Chem. Phys.* **1993**, *98*, 5648.

(13) (a) Andrae, D.; Häussermann, U.; Dolg, M.; Stoll, H.; Preuss, H. *Theor. Chim. Acta* **1990**, *77*, 123. (b) Dolg, M.; Wedig, U.; Stoll, H.; Preuss, H. *J. Chem. Phys.* **1987**, *86*, 866.

(14) (a) Zhao, Y.; Truhlar, D. G. *Theor. Chem. Acc.* **2008**, *120*, 215. (b) Zhao, Y.; Truhlar, D. G. *Acc. Chem. Res.* **2008**, *41*, 157. (c) Kulkarni, A. D.; Truhlar, D. G. *J. Chem. Theory Comput.* **2011**, *7*, 2325. (d) Zhao, Y.; Truhlar, D. G. *J. Chem. Theory Comput.* **2009**, *5*, 324.

(15) Marenich, A. V.; Cramer, C. J.; Truhlar, D. G. *J. Phys. Chem. B* **2009**, *113*, 6378.

(16) (a) Liu, P.; Xu, X.; Dong, X.; Keitz, B. K.; Herbert, M. B.; Grubbs, R. H.; Houk, K. N. *J. Am. Chem. Soc.* **2012**, *134*, 1464. (b) Herbert, M. B.; Lan, Y.; Keitz, B. K.; Liu, P.; Endo, K.; Day, M. W.; Houk, K. N.; Grubbs, R. H. *J. Am. Chem. Soc.* **2012**, *134*, 7861. (c) Giri, R.; Lan, Y.; Liu, P.; Houk, K. N.; Yu, J.-Q. *J. Am. Chem. Soc.* **2012**, *134*, 14118. (d) Miyazaki, H.; Herbert, M. B.; Liu, P.; Dong, X.; Xu, X.; Keitz, B. K.; Ung, T.; Mkrtumyan, G.; Houk, K. N.; Grubbs, R. H. *J. Am. Chem. Soc.* **2013**, *135*, 5848. (e) Xu, X.; Liu, P.; Shu, X.-z.; Tang, W.; Houk, K. N. *J. Am. Chem. Soc.* **2013**, *135*, 9271. (f) Cannon, J. S.; Zou, L.; Liu, P.; Lan, Y.; O'Leary, D. J.; Houk, K. N.; Grubbs, R. H. *J. Am. Chem. Soc.* **2014**, *136*, 6733. (g) Haynes, M. T.; Liu, P.; Baxter, R. D.; Nett, A. J.; Houk, K. N.; Montgomery, J. *J. Am. Chem. Soc.* **2014**, *136*, 17495. (h) Lu, G.; Fang, C.; Xu, T.; Dong, G.; Liu, P. *J. Am. Chem. Soc.* **2015**, *137*, 8274.

(17) (a) Tang, S.-Y.; Guo, Q.-X.; Fu, Y. *Chem. - Eur. J.* **2011**, *17*, 13866. (b) Gellrich, U.; Seiche, W.; Keller, M.; Breit, B. *Angew. Chem., Int. Ed.* **2012**, *51*, 11033. (c) Ariafard, A.; Asadollah, E.; Ostadebrahim, M.; Rajabi, N. A.; Yates, B. F. *J. Am. Chem. Soc.* **2012**, *134*, 16882. (d) Dang, Y.; Qu, S.; Wang, Z.-X.; Wang, X. *J. Am. Chem. Soc.* **2014**,

DOI: 10.1021/jacs.5b12112
J. Am. Chem. Soc. 2016, 138, 2712−2723

136, 986. (e) Dang, Y.; Qu, S.; Tao, Y.; Deng, X.; Wang, Z.-X. *J. Am. Chem. Soc.* **2015**, *137*, 6279.
(18) Harvey, J. N.; Aschi, M.; Schwarz, H.; Koch, W. *Theor. Chem. Acc.* **1998**, *99*, 95.
(19) Frisch, M. J.; Trucks, G. W.; Schlegel, H. B.; Scuseria, G. E.; Robb, M. A.; Cheeseman, J. R.; Scalmani, G.; Barone, V.; Mennucci, B.; Petersson, G. A.; Nakatsuji, H.; Caricato, M.; Li, X.; Hratchian, H. P.; Izmaylov, A. F.; Bloino, J.; Zheng, G.; Sonnenberg, J. L.; Hada, M.; Ehara, M.; Toyota, K.; Fukuda, R.; Hasegawa, J.; Ishida, M.; Nakajima, T.; Honda, Y.; Kitao, O.; Nakai, H.; Vreven, T.; Montgomery, J. A., Jr.; Peralta, J. E.; Ogliaro, F.; Bearpark, M.; Heyd, J. J.; Brothers, E.; Kudin, K. N.; Staroverov, V. N.; Kobayashi, R.; Normand, J.; Raghavachari, K.; Rendell, A.; Burant, J. C.; Iyengar, S. S.; Tomasi, J.; Cossi, M.; Rega, N.; Millam, N. J.; Klene, M.; Knox, J. E.; Cross, J. B.; Bakken, V.; Adamo, C.; Jaramillo, J.; Gomperts, R.; Stratmann, R. E.; Yazyev, O.; Austin, A. J.; Cammi, R.; Pomelli, C.; Ochterski, J. W.; Martin, R. L.; Morokuma, K.; Zakrzewski, V. G.; Voth, G. A.; Salvador, P.; Dannenberg, J. J.; Dapprich, S.; Daniels, A. D.; Farkas, Ö.; Foresman, J. B.; Ortiz, J. V.; Cioslowski, J.; Fox, D. J. *Gaussian 09*, revision A.01; Gaussian, Inc.: Wallingfor, CT, 2009.
(20) (a) Wilke, G.; Schott, H.; Heimbach, P. *Angew. Chem., Int. Ed. Engl.* **1967**, *6*, 92. (b) Amatore, C.; Aziz, S.; Jutand, A.; Meyer, G.; Cocolios, P. *New J. Chem.* **1995**, *19*, 1047. (c) Adamo, C.; Amatore, C.; Ciofini, I.; Jutand, A.; Lakmini, H. *J. Am. Chem. Soc.* **2006**, *128*, 6829. (d) Cai, X.; Majumdar, S.; Fortman, G. C.; Cazin, C. S. J.; Slawin, A. M. Z.; Lhermitte, C.; Prabhakar, R.; Germain, M. E.; Palluccio, T.; Nolan, S. P.; Rybak-Akimova, E. V.; Temprado, M.; Captain, B.; Hoff, C. D. *J. Am. Chem. Soc.* **2011**, *133*, 1290. (e) Ingram, A. J.; Walker, K. L.; Zare, R. N.; Waymouth, R. M. *J. Am. Chem. Soc.* **2015**, *137*, 13632.
(21) (a) Stahl, S. S.; Thorman, J. L.; Nelson, R. C.; Kozee, M. A. *J. Am. Chem. Soc.* **2001**, *123*, 7188. (b) Konnick, M. M.; Guzei, I. A.; Stahl, S. S. *J. Am. Chem. Soc.* **2004**, *126*, 10212. (c) Konnick, M. M.; Gandhi, B. A.; Guzei, I. A.; Stahl, S. S. *Angew. Chem., Int. Ed.* **2006**, *45*, 2904. (d) Konnick, M. M.; Stahl, S. S. *J. Am. Chem. Soc.* **2008**, *130*, 5753.
(22) (a) Landis, C. R.; Morales, C. M.; Stahl, S. S. *J. Am. Chem. Soc.* **2004**, *126*, 16302. (b) Popp, B. V.; Wendlandt, J. E.; Landis, C. R.; Stahl, S. S. *Angew. Chem., Int. Ed.* **2007**, *46*, 601. (c) Popp, B. V.; Stahl, S. S. *J. Am. Chem. Soc.* **2007**, *129*, 4410. (d) Popp, B. V.; Stahl, S. S. *Chem. - Eur. J.* **2009**, *15*, 2915. (e) Popp, B. V.; Morales, C. M.; Landis, C. R.; Stahl, S. S. *Inorg. Chem.* **2010**, *49*, 8200. (f) Konnick, M. M.; Decharin, N.; Popp, B. V.; Stahl, S. S. *Chem. Sci.* **2011**, *2*, 326. (g) Decharin, N.; Popp, B. V.; Stahl, S. S. *J. Am. Chem. Soc.* **2011**, *133*, 13268.
(23) (a) Keith, J. M.; Nielsen, R. J.; Oxgaard, J.; Goddard, W. A., III. *J. Am. Chem. Soc.* **2005**, *127*, 13172. (b) Keith, J. M.; Muller, R. P.; Kemp, R. A.; Goldberg, K. I.; Goddard, W. A., III.; Oxgaard, J. *Inorg. Chem.* **2006**, *45*, 9631. (c) Keith, J. M.; Goddard, W. A., III.; Oxgaard, J. *J. Am. Chem. Soc.* **2007**, *129*, 10361. (d) Keith, J. M.; Goddard, W. A., III. *J. Am. Chem. Soc.* **2009**, *131*, 1416. (e) Keith, J. M.; Goddard, W. A., III. *Organometallics* **2012**, *31*, 545.
(24) (a) Lapointe, D.; Fagnou, K. *Chem. Lett.* **2010**, *39*, 1118. (b) Balcells, D.; Clot, E.; Eisenstein, O. *Chem. Rev.* **2010**, *110*, 749.
(25) (a) Davies, D. L.; Donald, S. M. A.; Macgregor, S. A. *J. Am. Chem. Soc.* **2005**, *127*, 13754. (b) Lafrance, M.; Fagnou, K. *J. Am. Chem. Soc.* **2006**, *128*, 16496. (c) García-Cuadrado, D.; Braga, A. A. C.; Maseras, F.; Echavarren, A. M. *J. Am. Chem. Soc.* **2006**, *128*, 1066. (d) García-Cuadrado, D.; de Mendoza, P.; Braga, A. A. C.; Maseras, F.; Echavarren, A. M. *J. Am. Chem. Soc.* **2007**, *129*, 6880. (e) Lafrance, M.; Gorelsky, S. I.; Fagnou, K. *J. Am. Chem. Soc.* **2007**, *129*, 14570. (f) Gorelsky, S. I.; Lapointe, D.; Fagnou, K. *J. Am. Chem. Soc.* **2008**, *130*, 10848. (g) Rousseaux, S.; Gorelsky, S. I.; Chung, B. K. W.; Fagnou, K. *J. Am. Chem. Soc.* **2010**, *132*, 10692. (h) Zhang, S.; Shi, L.; Ding, Y. *J. Am. Chem. Soc.* **2011**, *133*, 20218. (i) Musaev, D. G.; Kaledin, A.; Shi, B.-F.; Yu, J.-Q. *J. Am. Chem. Soc.* **2012**, *134*, 1690. (j) Sanhueza, I. A.; Wagner, A. M.; Sanford, M. S.; Schoenebeck, F. *Chem. Sci.* **2013**, *4*, 2767. (k) Yang, Y.-F.; Cheng, G.-J.; Liu, P.; Leow, D.; Sun, T.-Y.; Chen, P.; Zhang, X.; Yu, J.-Q.; Wu, Y.-D.; Houk, K. N. *J. Am. Chem. Soc.* **2014**, *136*, 344. (l) Cheng, G.-J.; Yang, Y.-F.; Liu, P.; Chen, P.; Sun, T.-Y.; Li, G.; Zhang, X.; Houk, K. N.; Yu, J.-Q.; Wu, Y.-D. *J. Am. Chem. Soc.* **2014**, *136*, 894. (m) Anand, M.; Sunoj, R. B.; Schaefer, H. F., III *J. Am. Chem. Soc.* **2014**, *136*, 5535. (n) Haines, B. E.; Musaev, D. G. *ACS Catal.* **2015**, *5*, 830. (o) Dang, Y.; Qu, S.; Nelson, J. W.; Pham, H. D.; Wang, Z.-X.; Wang, X. *J. Am. Chem. Soc.* **2015**, *137*, 2006. (p) Haines, B. E.; Xu, H.; Verma, P.; Wang, X.-C.; Yu, J.-Q.; Musaev, D. G. *J. Am. Chem. Soc.* **2015**, *137*, 9022.
(26) (a) Lang, S. *Chem. Soc. Rev.* **2013**, *42*, 4867. (b) Chakrabarty, S.; Choudhary, S.; Doshi, A.; Liu, F.-Q.; Mohan, R.; Ravindra, M. P.; Shah, D.; Yang, X.; Fleming, F. F. *Adv. Synth. Catal.* **2014**, *356*, 2135. (c) Boyarskiy, V. P.; Bokach, N. A.; Luzyanin, K. V.; Kukushkin, V. Y. *Chem. Rev.* **2015**, *115*, 2698. (d) Kruithof, A.; Ruijter, E.; Orru, R. V. A. *Chem. - Asian J.* **2015**, *10*, 508.
(27) The energy release of the disproportionation (i.e., $H_2O_2 \rightarrow H_2O + 1/2\ O_2$) was not included.
(28) (a) Guimond, N.; Gouliaras, C.; Fagnou, K. *J. Am. Chem. Soc.* **2010**, *132*, 6908. (b) Guimond, N.; Gorelsky, S. I.; Fagnou, K. *J. Am. Chem. Soc.* **2011**, *133*, 6449. (c) Wang, G.-W.; Yuan, T.-T.; Li, D.-D. *Angew. Chem., Int. Ed.* **2011**, *50*, 1380. (d) Karthikeyan, J.; Cheng, C.-H. *Angew. Chem., Int. Ed.* **2011**, *50*, 9880. (e) Xu, L.; Zhu, Q.; Huang, G.; Cheng, B.; Xia, Y. *J. Org. Chem.* **2012**, *77*, 3017.
(29) (a) Hyster, T. K.; Rovis, T. *J. Am. Chem. Soc.* **2010**, *132*, 10565. (b) Kim, H.; Shin, K.; Chang, S. *J. Am. Chem. Soc.* **2014**, *136*, 5904. (c) Park, J.; Chang, S. *Angew. Chem., Int. Ed.* **2015**, *54*, 14103. (d) Shin, K.; Park, S.-W.; Chang, S. *J. Am. Chem. Soc.* **2015**, *137*, 8584.
(30) (a) Gao, K.; Yoshikai, N. *J. Am. Chem. Soc.* **2011**, *133*, 400. (b) Yang, Z.; Yu, H.; Fu, Y. *Chem. - Eur. J.* **2013**, *19*, 12093. (c) Zhou, B.; Chen, H.; Wang, C. *J. Am. Chem. Soc.* **2013**, *135*, 1264. (d) Topczewski, J. J.; Sanford, M. S. *Chem. Sci.* **2015**, *6*, 70 and references therein. (e) Wang, Z.; Kuninobu, Y.; Kanai, M. *J. Am. Chem. Soc.* **2015**, *137*, 6140.

DOI: 10.1021/jacs.5b12112
J. Am. Chem. Soc. 2016, 138, 2712−2723